derived from the mild acidolysis of poplar in the region of δ_C/δ_H 98–104/4.5–5.0 ppm, and these correlations were assigned to C_1-H_1 bonds of the phenyl glycoside type LC linkages. Miyagawa et al. (2013) reported correlations at δ_C/δ_H 98.6/4.97 ppm in the 2D HSQC spectrum of a fraction from the MWL residue of eucalyptus that were assigned to the $C_{1\beta}$-$H_{1\beta}$ bonds of the phenyl glycoside type LC linkages. The assignment of correlations of this particular type, however, remains speculative, because there has not been enough 2D HSQC NMR data (i.e., both ^{1}H and ^{13}C NMR data) collected for synthetic phenyl glycoside type LCC model compounds to allow for accurate assignments. Indeed, there is only a limited set of data available concerning synthetic phenyl glycoside type LCC model compounds, including several monolignol glucosides (i.e., coniferin, syringin and *p*-glucocoumaryl alcohol) (Terashima et al. 1996; Daubresse et al. 1998; Ralph et al. 2004), and dihydroconiferin (Mazur et al. 2007). Although several coniferyl alcohol β-glycosides have been synthesised, including glucoside, galactoside and fucoside (Delay et al. 1994), and the monolignol and dilignol glucosides have been isolated from the leaves of *Pinus contorta* subsp. *contorta* (Higuchi et al. 1977), only their ^{1}H NMR data have been reported. In contrast, large amounts of data have been published for native lignan glycosides (Sugiyama et al. 1993; Jin et al. 1999; Kamel 2003; Machida et al. 2009; Yuan et al. 2011b), although differences in the conditions under which the NMR measurements were collected have diminished the overall usefulness of these data, and they are consequently not suitable for the analysis of phenyl glyoside-type LCCs. The systematic collection of fundamental data for the correlations between the ^{1}H and ^{13}C signals from the 2D HSQC spectra of phenyl glycoside type LCC model compounds is therefore strongly desired.

Herein, a series of monolignol β-glycosides with different sugar moieties were selected as phenyl glycoside type LCC model compounds (Figure 1), because NMR data of monolignol β-glucosides have been used for the assignment of the signals for phenyl glycoside type LC linkages in previous papers (Balakshin et al. 2011; Yuan et al. 2011a; Miyagawa et al. 2013), and dihydromonolignol and *p*-hydroxybenzaldehyde derivative β-glycosides which are also useful LCC model compounds with C_α-C_β saturated substructures and C_α-oxidised substructures, respectively, are easily obtained. This paper describes the syntheses of monolignol β-glycosides (compounds **1G**, **1S**, **1H**, **2G**, **2S**, **2H**, **3G**, **3S**, **3H**, **4G**, **4S** and **4H**), dihydromonolignol β-glycosides (compounds **5G**, **5S**, **5H**, **6G**, **6S**, **6H**, **7G**, **7S**, **7H**, **8G**, **8S** and **8H**) and *p*-hydroxybenzaldehyde derivative β-glycosides (compounds **9G**, **9S**, **9H**, **10G**, **10S**, **10H**, **11G**, **11S**, **11H**, **12G**, **12S** and **12H**) shown in Figure 1, and the subsequent acquisition of their NMR data, in what we believe will be the first step towards the accumulation of fundamental HSQC NMR data for the analysis of phenyl glycoside type LCCs.

Materials and methods

Coniferin (**1G**), syringin (**1S**) and *p*-glucocoumaryl alcohol (**1H**) were synthesised according to the method reported by Terashima et al. (1996) (Figure 2). All of the starting materials were obtained from commercial suppliers and used without further purification. Compound purifications were performed by silica gel column chromatography i.e., 60 N silica gel (spherical, neutral, 100–210 μm, Kanto Chemical Company, Tokyo, Japan). Silica gel plates (Silica gel 60 F254, 0.25 mm

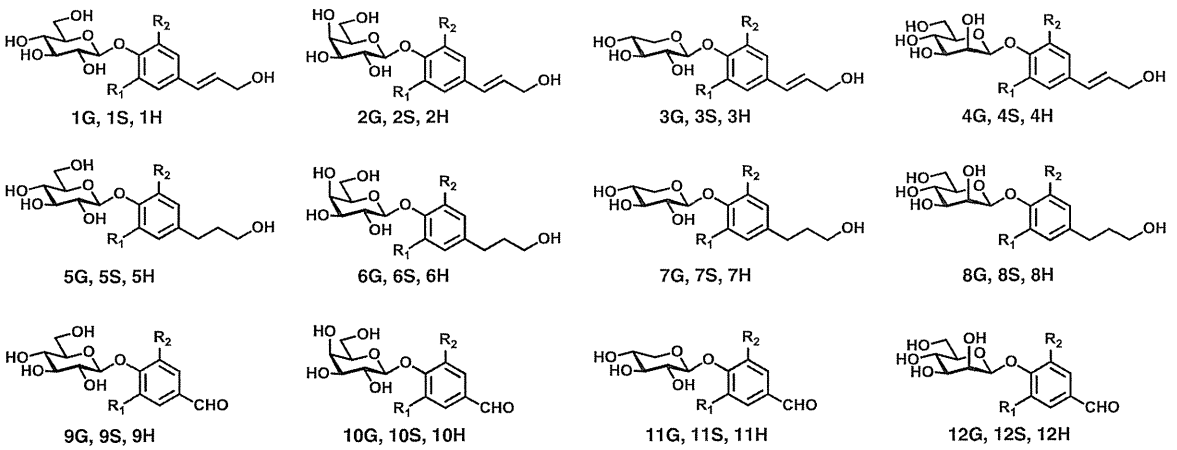

G: R_1=OMe, R_2=H, **S**: R_1=R_2=OMe, **H**: R_1=R_2=H

Figure 1 Phenyl glycoside type LCC model compounds in the current study.

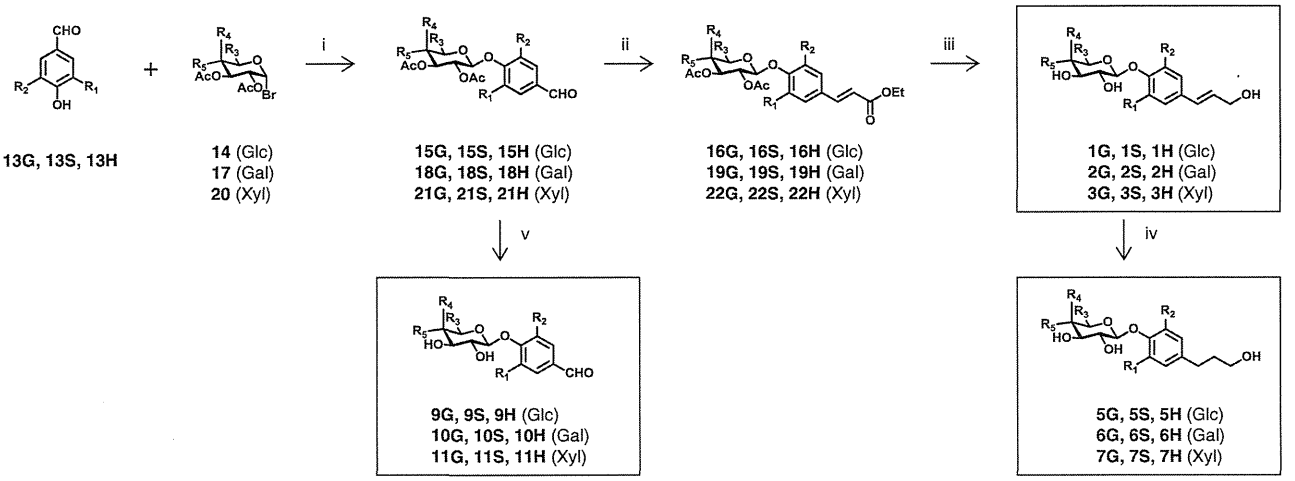

G: R_1=OMe, R_2=H **S**: R_1=R_2=OMe **H**: R_1=R_2=H

1, 5, 9 (Glc): R_3=CH_2OH, R_4=H, R_5=OH
2, 6, 10 (Gal): R_3=CH_2OH, R_4=OH, R_5=H
3, 7, 11 (Xyl): R_3=R_4=H, R_5=OH

14, 15, 16 (Glc): R_3=CH_2OAc, R_4=H, R_5=OAc
17, 18, 19 (Gal): R_3=CH_2OAc, R_4=OAc, R_5=H
20, 21, 22 (Xyl): R_3=R_4=H, R_5=OAc

i) Ag_2O/quinoline/r.t./1.5 h
ii) Monoethyl malonic acid/pyridine/piperidine/100°C/1.5 h
iii) DIBAL-H/dry toluene/0°C/1 h
iv) H_2/Pd-C/MeOH/r.t./1.5 h
v) NaOMe/MeOH/r.t./1 h

Figure 2 Synthetic route for 1,2-*trans* glycosides (β-glucosides, β-galactosides and β-xylosides) with different lignin moieties (monolignol, dihydromonolignol and *p*-hydroxybenzaldehyde derivative).

thickness, Merck, Darmstadt, Germany) served for preparative TLC purification (PTLC). The ^1H and ^{13}C NMR spectra were recorded on a Varian 500 FT-NMR (500 MHz) spectrometer (Agilent Technologies, Santa Clara, CA, USA). The NMR samples were prepared in $CDCl_3$ or DMSO-d_6, with the residual solvent peak as the internal reference. The chemical shifts (δ) and coupling constants (J) are given in ppm and Hz, respectively. All of the peaks in the spectra were assigned by gCOSY, NOESY, gHSQC and gHMBC spectroscopy. Melting points (m.p.) were measured in a micro melting point apparatus (Yanagimoto seisakusho, Kyoto, Japan). Optical rotations were measured with a JASCO Dip-1000 digital polarimeter (Tokyo, Japan).

Koenig-Knorr glycosylation

4-(2′,3′,4′,6′-Tetra-*O*-acetyl-β-D-galactopyranosyloxy)-3-methoxybenzaldehyde (**18G**). Vanillin (**13G**) (547.7 mg, 3.6 mmol) and 2,3,4,6-tetra-*O*-acetyl-α-D-galactopyranosyl bromide (**17**) (Pieber et al. 2010) (1.49 g, 3.6 mmol) were dissolved in quinoline (10 ml) at 0°C. Ag_2O (834.2 mg, 3.6 mmol) was then added with vigorous stirring, and the resulting mixture was stirred at ambient temperature for 1.5 h. The reaction mixture was then passed through a pad of celite (Celite® 535RVS, Nacalai, Kyoto, Japan), and the filtrate was collected and extracted with EtOAc. The EtOAc extract was then washed sequentially with a 1 M HCl solution, a saturated aqueous $NaHCO_3$ solution, and brine, before being dried over anhydrous Na_2SO_4, and evaporated to give the crude product. The crude product was then purified by silica gel column chromatography using an EtOAc/*n*-hexane eluent (1:2 to 1:1 – v/v) to give compound **18G** as viscous oil (1.70 g, 97.7% yield).

Compounds **18S**, **18H**, **21G**, **21S**, and **21H** were prepared according to the procedure described above for the preparation of **18G** in yields of 99.1, 34.2, 96.3, 52.8 and 58.2%, respectively.

Knoevenagel condensation

(*E*)-1-Ethoxy-3-[3-methoxy-4-(2′,3′,4′,6′-tetra-*O*-acetyl-β-D-galactopyranosyloxy) phenyl]-2-propene-1-one (**19G**). Compound **18G** (1.08 g, 2.2 mmol) and monoethyl malonic acid (Hediger 2004) (384.2 mg, 2.9 mmol) were dissolved in a mixture of pyridine (6 ml) and piperidine (0.1 ml), and the resulting solution was stirred at 100°C for 1.5 h. The mixture was then evaporated to dryness to give crude the product, which was purified by a silica gel column chromatography with EtOAc/*n*-hexane (2:1 – v/v) as eluent to give compound **19G** as an off-white crystalline solid (1.12 g, 96.2% yield).

Compounds **19S**, **19H**, **22G**, **22S** and **22H** were prepared according to the procedure described above for the preparation of **19G**, except the purifications by column chromatography were performed with a mixture of EtOAc/*n*-hexane (1:1 – v/v) as eluent for **22G**, **22S** and **22H**. The products were isolated in yields of 97.0, 52.2, 76.5, 70.9 and 81.6%, respectively.

Reduction with DIBAL-H

(*E*)-3-[3-Methoxy-4-(β-D-galactopyranosyloxy) phenyl]-2-propene-1-ol (**2G**). Diisobutylaluminum hydride (DIBAL-H) (1 M in toluene, 10.4 ml, 10.4 mmol) was added in a drop-wise manner to a solution compound **19G** (552.7 mg, 1.1 mmol) in dry toluene (15 ml) at 0°C over a period of 10 min, and the resulting solution was stirred at 0°C for 1 h. The excess DIBAL-H was then quenched via the slow addition of EtOH (20 ml) to the reaction flask, and the resulting mixture was stirred at 0°C for 30 min. The solvents were then removed in vacuo to give a white powder, which was suspended in boiling water and filtered. This suspension and filtration process was repeated three times in total. The combined filtrates were evaporated to the give crude product, which was recrystallised from EtOH of give compound **2G** as white crystals (191.3 mg, 52.6% yield).

Table 1 ^{1}H, ^{13}C NMR, m.p. and optical rotations data of monolignol β-glycosides.

	1G	1S	1H	2G	2S	2H	3G	3S	3H	4G	4S	4H
^{1}H-NMR (ppm)												
H1	4.88 d (7.5)	4.91 d (7.5)	4.84 d (7.5)	4.84 d (7.5)	4.82 d (7.5)	4.80 d (7.5)	4.87 d (7.0)	4.93 d (6.5)	4.84 d (7.5)	5.01 s	4.86 d (0.5)	5.12 s
H2	3.22–3.31	3.17–3.21	3.20–3.27	3.50–3.58	3.46–3.52	3.52–3.57	3.18–3.25	3.27 m	3.19–3.37	3.84 d (4.0)	3.84 s	3.83 dd (1.5, 5.0)
H3	3.22–3.31	3.03 m	3.20–3.27	3.40–3.47	3.46–3.52	3.40 m	3.18–3.25	3.22 dd (5.0, 8.0)	3.19–3.37	3.38–3.50	3.26 dd (3.0, 9.0)	3.38–3.42
H4	3.16 m	3.13 m	3.15 m	3.69 t (4.0)	3.65 t (4.0)	3.69 t (4.0)	3.30–3.35	3.30–3.38	3.19–3.37	3.38–3.50	3.33–3.38	3.38–3.42
H5a	3.22–3.31	3.17–3.21	3.20–3.27	3.51–3.56	3.25 t (6.5)	3.52–3.57	3.18–3.25	2.98 dd (4.0, 11.5)	3.19–3.37	3.18 m	2.98 m	3.23 m
H5b	–	–	–	–	–	–	3.71 dd (5.5, 11.5)	3.75–3.77	3.73 dd (5.0, 11.0)	–	–	–
H6a	3.44 dt (5.5, 12.0)	3.40 dt (5.5, 11.5)	3.46 dt (6.0, 11.5)	3.51–3.56	3.33 m	3.48 m	–	–	–	3.38–3.50	3.45 dd (6.0, 11.5)	3.45 m
H6b	3.66 m	3.59 m	3.69 m	3.44–3.48	3.46–3.52	3.52–3.57	–	–	–	3.70 m	3.65 d (11.5)	3.71 m
Hα	6.47 d (16.0)	6.46 d (16.0)	6.48 d (16.0)	6.46 d (16.0)	6.46 d (16.0)	6.48 d (16.0)	6.46 d (16.0)	6.47 d (15.5)	6.48 d (16.5)	6.47 d (16.0)	6.46 d (16.0)	6.48 d (16.0)
Hβ	6.28 d (5.0, 15.5)	6.34 dt (5.5, 16.0)	6.24 dt (5.5, 16.0)	6.27 dt (5.5, 16.0)	6.33 dt (5.0, 15.5)	6.24 dt (5.0, 16.0)	6.28 dt (5.0, 16.0)	6.34 dt (5.0, 15.5)	6.23 dt (5.0, 16.0)	6.28 dt (5.0, 15.5)	6.36 dt (5.0, 16.0)	6.23 dt (5.0, 16.0)
Hγ	4.09 dt (2.0, 5.5)	4.10 m	4.08 dd (3.5, 5.0)	4.09 dt (1.5, 5.5)	4.10 dt (1.0, 5.0)	4.09 dt (1.5, 5.5)	4.09 dt (2.0, 5.5)	4.11 dt (1.5, 5.0)	4.08 dt (1.5, 5.5)	4.09 dt (1.0, 5.0)	4.11 d (4.5)	4.08 m
H2′	7.06 d (1.5)	6.73 s	7.34 dt (3.0, 8.5)	7.05 d (2.0)	6.72 s	7.34 dt (2.5, 9.0)	7.06 d (2.0)	6.71 s	7.34 dt (3.0, 8.5)	7.06 d (2.0)	6.75 s	7.34 dt (2.0, 8.5)
H3′	–	–	6.97 dt (2.5, 9.0)	–	–	6.97 dt (2.5, 9.0)	–	–	6.95 dt (2.5, 9.0)	–	–	6.95 dt (2.5, 9.0)
H5′	7.01 d (8.0)	–	6.97 dt (2.5, 9.0)	7.01 d (8.5)	–	6.97 dt (2.5, 9.0)	6.97 d (8.5)	–	6.95 dt (2.5, 9.0)	7.03 d (8.0)	–	6.95 dt (2.5, 9.0)
H6′	6.89 dd (1.5, 8.5)	6.73 s	7.34 dt (3.0, 8.5)	6.89 dd (2.0, 8.5)	6.72 s	7.34 dt (2.5, 9.0)	6.89 dd (2.0, 8.5)	6.71 s	7.34 dt (3.0, 8.5)	6.88 dd (2.0, 8.5)	6.75 s	7.34 dt (2.0, 8.5)
-OMe	3.78 s	3.77 s	–	3.78 s	3.75 s	–	3.77 s	3.76 s	–	3.78 s	3.79 s	–
^{13}C-NMR (ppm)												
C1	100.0	102.5	100.3	100.7	103.4	101.0	100.8	102.7	100.8	98.7	101.6	97.7
C2	73.2	74.2	73.2	70.3	71.4	70.3	73.0	73.2	73.1	70.5	70.2	70.5
C3	77.0	77.2	77.0	73.6	73.2	73.3	76.5	75.4	76.4	73.5	73.4	73.4
C4	69.6	70.4	69.7	68.2	68.3	73.7	69.3	69.5	69.4	66.9	66.8	66.8
C5	76.8	76.5	76.6	75.5	75.9	75.5	65.7	65.4	65.7	77.7	77.9	77.7
C6	60.6	60.9	60.7	60.4	60.5	60.7	–	–	–	61.1	61.3	61.0
Cα	128.4	128.4	128.1	128.9	128.5	128.1	128.3	128.5	128.5	128.4	128.3	128.1

(**Table 1** Continued)

	1G	1S	1H	2G	2S	2H	3G	3S	3H	4G	4S	4H
Cβ	129.0	130.2	128.8	129.4	130.2	128.8	129.2	130.3	129.4	129.2	130.5	128.7
Cγ	61.6	61.4	61.6	61.7	61.5	61.6	61.6	61.5	61.6	61.6	61.4	61.6
C1′	130.1	132.6	130.7	131.0	132.7	130.6	131.4	132.9	130.8	131.4	133.2	130.5
C2′	109.8	105.0	127.2	110.0	104.5	127.2	109.9	103.8	127.2	109.8	104.1	127.2
C3′	149.0	152.7	116.3	149.1	152.8	116.3	149.3	152.9	116.4	149.3	152.8	116.1
C4′	146.0	133.8	156.7	146.1	134.1	156.8	145.5	132.9	156.4	145.9	133.9	156.4
C5′	119.0	152.7	116.3	115.3	152.8	116.3	115.9	152.9	116.4	116.6	152.8	116.1
C6′	115.2	105.0	127.2	119.0	104.5	127.2	118.9	103.8	127.2	119.0	104.1	127.2
-OMe	55.6	56.3	–	55.7	56.4	–	55.6	56.1	–	55.6	56.3	–
m.p. (°C)	185–188	191–192	153–155	201–204	186–189	187–189	136–137	124–125	192–196	168–171	n.m.	n.m.
Optical rotation												
$[\alpha]_D$	-58.6	-20.6	-58.7	-48.2	-19.7	-47.0	-34.5	-38.7	-22.1	-60.5	-39.2	-67.8
T[a]	19.5	20.3	22.6	21.7	22.3	22.9	20.9	21.3	22.7	27.7	24.1	19.9
c[b]	1.1	1.0	0.2	1.0	1.1	0.6	0.7	0.8	0.2	0.4	0.3	0.6

Refer to Figure 1 for the structure abbreviations. The values in parentheses are coupling constants (*J*). d, doublet; t, triplet; dd, double doublet; dt, double triplet; m, multiplet; m.p., melting point; n.m., not measured because the compound was oily. [a]Temperature (°C). [b]Concentration (g/100 ml of MeOH).

Compounds **2S**, **2H**, **3G**, **3S** and **3H** were prepared according to the procedure described above for the preparation of **2G**, except compounds **3G**, **3S** and **3H** were recrystallised from a mixture of MeOH/CH_2Cl_2 (1:4 – v/v). These products were isolated in yields of 59.0, 10.4, 55.7, 14.6 and 72.3%, respectively. ^1H and ^{13}C NMR data, m.p. and optical rotations are summarised in Table 1.

Mitsunobu glycosylation

4-(2′,3′:4′,6′-Di-*O*-isopropylidene-β-D-mannopyranosyloxy)-3-methoxy-benzaldehyde (24G). 2′,3′:4′,6′-Di-*O*-isopropylidene-D-mannopyranose (**23**) (Cocinero et al. 2008) (260.1 mg, 1 mmol), vanillin (**3G**) (760.8 mg, 5 mmol), triphenylphosphine (1.31 g, 5 mmol) and powdered 4 Å molecular sieves (2 g) were placed in a flask and dried under vacuum overnight at ambient temperature. Dry toluene (20 ml) was added to the flask, and the resulting mixture was stirred for 10 min. Diisopropyl azodicarboxylate (DIAD; 95%, 1 ml, 5 mmol) was then added to the solution, and the resulting mixture was stirred at ambient temperature for 1.5 h. The mixture was filtered and the filtrate was washed sequentially with a 1 M aqueous NaOH solution, a saturated aqueous $NaHCO_3$ solution, and brine. The organic layer was then dried over anhydrous Na_2SO_4 and concentrated in vacuo to give the crude product, which was dissolved in a mixture of EtOAc and *n*-hexane (1:4 – v/v) before being held at -20°C overnight. The mixture was then filtered to remove the resulting white precipitate (triphenylphosphine oxide and diisopropyl hydrazine carboxylate), and concentrated. This purification process was repeated twice, and the resulting residue was purified by a silica gel column chromatography with EtOAc/*n*-hexane (1:4 – v/v) as eluent to give compound **24G** (209.6 mg, 53.7% yield) and the corresponding α-anomer (32.6 mg, 8.3% yield) as viscous colourless oils.

Compounds **24S** and **24H** were prepared according to the procedure described above for the preparation of **24G** in yields of 41.2 and 61.4%, respectively.

Knoevenagel condensation

(*E*)-1-Ethoxy-3-[3-methoxy-4-(2′,3′:4′,6′-di-*O*-isopropylidene-β-D-mannopyranosy-loxy)phenyl]-2-propene-1-one (**25G**). Compound **24G** (84.8 mg, 0.2 mmol) and monoethyl malonic acid (Hediger 2004) (37.3 mg, 0.3 mmol) were added to a mixture of pyridine (3 ml) and piperidine (0.05 ml), and the resulting solution was stirred at 100°C for 1.5 h. The mixture was then distilled to dryness to give the crude product, which was purified by silica gel column chromatography with EtOAc/*n*-hexane (1:2 – v/v) as eluent to give compound **25G** as a viscous colorless oil (51.3 mg, 50.2% yield).

Compounds **25S** and **25H** were prepared according to the procedure described above for the preparation of **25G** in yields of 72.6 and 59.8%, respectively.

Reduction with DIBAL-H

(*E*)-3-[3-Methoxy-4-(2′,3′:4′,6′-di-*O*-isopropylidene-β-D-mannopyranosyloxy)phenyl]-2-propene-1-ol (**26G**). DIBAL-H (1 M in toluene, 0.18 ml, 0.18 mmol) was added to a solution of compound **25G** (33.3 mg, 0.07 mmol) in dry toluene (1.5 ml) at 0°C, and the

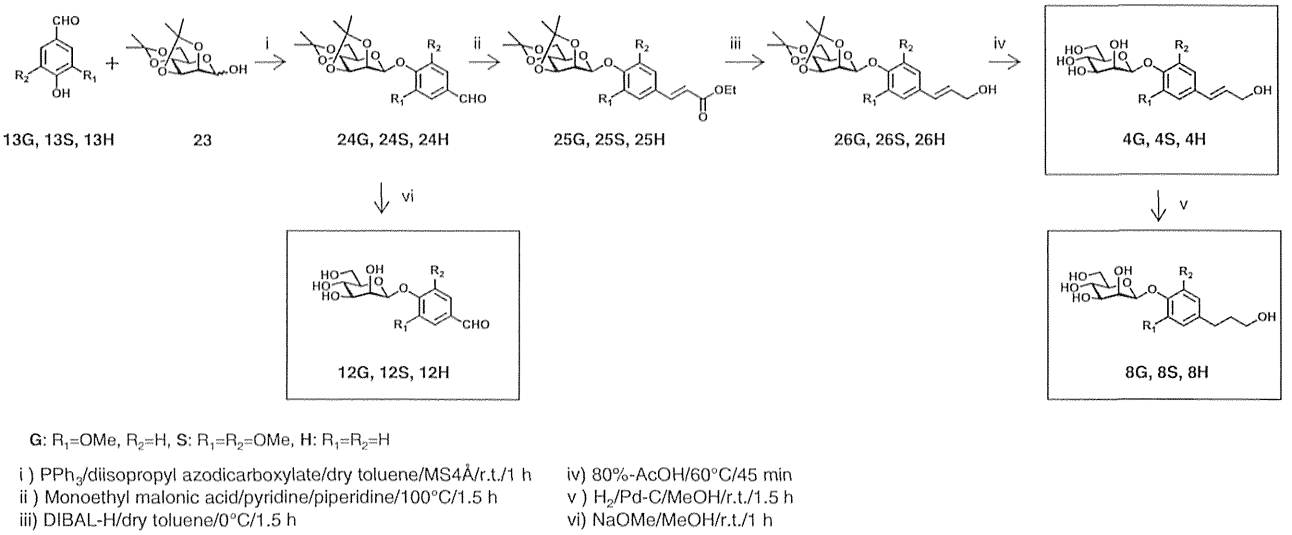

G: R_1=OMe, R_2=H, S: R_1=R_2=OMe, H: R_1=R_2=H

i) PPh_3/diisopropyl azodicarboxylate/dry toluene/MS4Å/r.t./1 h
ii) Monoethyl malonic acid/pyridine/piperidine/100°C/1.5 h
iii) DIBAL-H/dry toluene/0°C/1.5 h
iv) 80%-AcOH/60°C/45 min
v) H_2/Pd-C/MeOH/r.t./1.5 h
vi) NaOMe/MeOH/r.t./1 h

Figure 3 Synthetic route for 1,2-*cis* glycosides (β-mannosides) with different lignin moieties (monolignol, dihydromonolignol and *p*-hydroxybenzaldehyde derivative).

resulting solution was stirred at 0°C for 1 h. The excess DIBAL-H was then quenched via the cautious addition of EtOH (2 ml) to the reaction flask, and the resulting mixture was stirred at 0°C for 30 min. The mixture was then evaporated to dryness to give the crude product, which was purified by PTLC using EtOAc/*n*-hexane (1:1 – v/v) as the eluent to give compound **26G** as a viscous colourless oil (16.2 mg, 53.3% yield).

Compounds **26S** and **26H** were prepared according to the procedure described above for the preparation of **26G** in yields of 33.9 and 65.8% yields, respectively.

Deisopropylidenation

(*E*)-3-[3-Methoxy-4-(β-D-mannopyranosyloxy)phenyl]-2-propene-1-ol (4G). Compound **26G** (13.6 mg, 0.03 mmol) was dissolved in an 80% AcOH aqueous solution (v/v) (1 ml), and the resulting solution was stirred at 60°C for 45 min. The mixture was then concentrated to give the crude product, which was purified by PTLC using MeOH/CH_2Cl_2 (1:4 – v/v) as the eluent to afford compound **4G** as a colourless viscous oil (7.6 mg, 69.1% yield).

Compounds **4S** and **4H** were prepared according to the procedure described above for the preparation of **4G** in yields of 52.9 and 53.9%, respectively. ^{1}H and ^{13}C NMR data, m.p. and optical rotations are summarised in Table 1.

Catalytic hydrogenation

3-[3-Methoxy-4-(β-D-galactopyranosyloxy) phenyl]-propan-1-ol (**5G**). Palladium- activated on carbon (Pd 10%; Pd-C) was added to the solution of compound **1G** (20.0 mg, 0.06 mmol) in MeOH (1.5 ml). The reaction mixture was stirred at r.t. for 1 h under H_2. The reaction mixture was then passed through a pad of celite, and the filtrate was evaporated to dryness to give crude product which was purified by PTLC with MeOH/CH_2Cl_2 (1:4 – v/v) as eluent to give compound **5G** as a viscous colourless oil (7.5 mg, 81.6% yield).

Compounds **5S**, **5H**, **6G**, **6S**, **6H**, **7G**, **7S**, **7H**, **8G**, **8S** and **8H** were prepared according to the procedure described above for the preparation of **5G** in yields of 77.5, 76.0, 83.1, 86.6, 51.8, 57.3, 68.6, 53.5, 68.0, 76.4 and 66.3% yields, respectively. ^{1}H and ^{13}C NMR data and m.p. are summarised in Table 2.

Deacetylation

4-(β-D-Glucopyranosyloxy)-3-methoxy-benzaldehyde (**9G**). 28%NaOMe in MeOH was added into the solution of compound **15G** (12.1 mg, 0.03 mmol) in MeOH (1 ml) at 0°C. The resulting solution was stirred at r.t. for 1 h, neutralised with Amberlite 120B and filtered. The filtrate was evaporated to dryness to give the crude product, which was purified by PTLC with MeOH/CH_2Cl_2 (1:4 – v/v) as eluent to give compound **9G** as a white crystal (7.5 mg, 94.9% yield).

Compounds **9S**, **9H**, **10G**, **10S**, **10H**, **11G**, **11S** and **11H** were prepared according to the procedure described above for the preparation of **9G** in yields of 87.2, 98.6, 89.2, 86.0, 91.5, 97.2, 74.6 and 96.9% yields, respectively. ^{1}H and ^{13}C NMR data and m.p. are summarised in Table 3.

Deisopropylidenation

4-(β-D-Mannopyranosyloxy)-3-methoxy-benzaldehyde (**12G**). Compound **24G** (17.4 mg, 0.04 mmol) was dissolved in an 80% AcOH aqueous solution (v/v) (1 ml), and the resulting solution was stirred at 60°C for 1.75 h. The mixture was then concentrated to give the crude product, which was purified by PTLC with MeOH/CH_2Cl_2 (1:4 – v/v) as eluent to afford compound **12G** as a white crystal (13.7 mg, 98.8% yield).

Compounds **12S** and **12H** were prepared according to the procedure described above for the preparation of **12G**, except the

Table 2 ^{1}H, ^{13}C NMR and m.p. data of dihydromonolignol β-glycosides.

	5G	5S	5H	6G	6S	6H	7G	7S	7H	8G	8S	8H
^{1}H-NMR (ppm)												
H1	4.83 d (7.5)	4.82 d (7.0)	4.79 d (8.0)	4.79 d (8.0)	4.74 d (7.5)	4.75 d (8.0)	4.81 d (7.0)	4.88 d (7.0)	4.78 d (7.5)	4.93 s	4.81 d (5.0)	5.07 s
H2	3.22–3.27	3.18–3.20	3.19–3.24	3.57 dd (5.0, 7.5)	3.48–3.52	3.54–3.55	3.32–3.36	3.34–3.38	3.30–3.36	3.83 dd (2.0, 5.5)	3.82 t (3.0)	3.82 dd (1.5, 5.0)
H3	3.22–3.27	3.18–3.20	3.23–3.28	3.68 t (3.5)	3.65 t (3.5)	3.38–3.42	3.17–3.22	3.21 dd (5.0, 8.0)	3.19–3.22	3.38–3.42	3.25 m	3.37–3.42
H4	3.14 dt (5.0, 8.5)	3.13 dt (5.0, 9.0)	3.15 m	3.35–3.40	3.30–3.35	3.69 t (3.5)	3.20–3.24	3.26 ddd (5.0, 6.5, 8.0)	3.19–3.22	3.38–3.42	3.32–3.37	3.37–3.42
H5a	3.22–3.27	3.02 m	3.27–3.32	3.48–3.52	3.24 t (6.0)	3.54–3.55	3.166 t (11.5)	2.97 dd (8.0, 12.0)	3.19–3.22	3.15 m	3.98 m	3.21 m
H5b	–	–	–	–	–	–	3.70 dd (5.5, 11.5)	3.75 dd (5.0, 11.5)	3.72 dd (5.0, 11.5)	–	–	–
H6a	3.45 dd (6.0, 12.0)	3.40–3.44	3.45 dt (6.0, 11.5)	3.45 dd (4.0, 5.5)	3.42 dd (6.0, 11.5)	3.47 m	–	–	–	3.45 dt (6.0, 12.5)	3.45 dd (6.0, 7.0)	3.45 dd (5.5, 13.0)
H6b	3.66 m	3.59 m	3.68 m	3.50–3.55	3.48–3.53	3.54–3.55	–	–	–	3.69 m	3.66 m	3.70 m
Hα	2.53 t (7.5)	2.53 t (7.5)	2.54 t (7.5)	2.53 t (7.5)	2.53 t (7.5)	2.54 t (8.0)	2.53 t (7.0)	2.53 t (7.5)	2.54 t (7.5)	2.53 t (8.0)	2.54 t (8.0)	2.53 t (8.0)
Hβ	1.69 m	1.71 m	1.67 m	1.69 m	1.71 m	1.67 m	1.68 m	1.71 m	1.66 m	1.69 m	1.71 m	1.66 m
Hγ	3.40 dd (6.0, 12.0)	3.40–3.44	3.37–3.41	3.37–3.43	3.30–3.35	3.38–3.42	3.40 dd (6.5, 11.5)	3.42 dd (6.0, 11.5)	3.38 dd (6.5, 11.5)	3.38–3.42	3.40–3.44	3.37–3.42
H2′	6.80 d (2.0)	6.49 s	7.09 d (8.5)	6.80 d (2.0)	6.49 s	7.09 d (9.0)	6.80 d (2.0)	6.48 s	7.09 d (7.5)	6.81 d (2.0)	6.51 s	7.09 d (9.0)
H3′	–	–	6.93 d (9.0)	–	–	6.92 d (8.5)	–	–	6.90 d (7.5)	–	–	6.90 d (8.5)
H5′	6.97 d (8.0)	–	6.93 d (9.0)	7.00 d (8.5)	–	6.92 d (8.5)	6.92 d (8.5)	–	6.90 d (7.5)	6.99 d (8.5)	–	6.90 d (8.5)
H6′	6.66 dd (2.0, 8.0)	6.49 s	7.09 d (8.5)	6.66 dd (2.0, 8.5)	6.49 s	7.09 d (9.0)	6.67 dd (2.0, 8.0)	6.48 s	7.09 d (7.5)	6.66 dd (2.0, 8.0)	6.51 s	7.09 d (9.0)
-OMe	3.74 s	3.73 s	–	3.74 s	3.72 s	–	3.74 s	3.72 s	–	3.75 s	3.75 s	–
^{13}C-NMR (ppm)												
C1	100.3	102.9	100.6	101.0	103.7	101.2	101.3	102.8	101.2	99.0	101.7	97.9
C2	73.3	74.2	73.3	70.3	71.4	70.3	69.4	69.5	69.4	70.5	70.1	70.5
C3	76.9	76.5	76.6	68.1	67.8	73.3	76.5	75.4	76.5	73.5	73.4	73.5
C4	69.7	69.9	69.7	73.5	73.2	68.1	73.1	73.2	73.1	66.9	66.8	66.9
C5	77.0	77.2	77.0	75.4	75.4	75.4	65.6	65.3	65.6	77.7	77.8	77.6
C6	60.7	60.9	60.7	60.4	60.1	60.4	–	–	–	61.1	61.3	61.1
Cα	31.2	31.9	30.8	31.3	31.9	30.8	31.3	32.0	30.8	31.3	32.0	30.8

(Table 2 Continued)

	5G	5S	5H	6G	6S	6H	7G	7S	7H	8G	8S	8H
Cβ	34.5	34.2	34.5	34.5	37.3	34.5	34.5	34.3	34.5	34.4	34.3	34.5
Cγ	60.1	60.2	60.0	60.2	60.2	60.0	60.1	60.2	60.0	60.1	60.2	60.0
C1′	135.9	137.9	135.4	135.9	137.9	135.3	136.5	138.2	135.5	136.5	138.5	135.2
C2′	112.8	106.5	129.1	112.9	106.5	129.0	112.9	105.9	129.1	112.8	106.2	129.1
C3′	148.8	152.4	116.1	148.9	152.5	116.1	149.2	152.6	116.3	149.2	152.5	115.8
C4′	144.6	132.6	155.5	144.7	132.7	155.6	144.1	131.5	155.2	144.4	132.5	155.2
C5′	115.4	152.4	116.1	115.5	152.5	116.1	116.3	152.6	116.3	117.1	152.5	115.8
C6′	120.1	106.5	129.1	120.1	106.5	129.0	120.1	105.9	129.1	120.1	106.2	129.1
-OMe	55.6	56.3	–	55.7	56.3	–	55.6	56.0	–	55.6	56.3	–
m.p. (°C)	113–116	148–150	n.m.	142–145	117–121	n.m.	125–131	147–149	171–174	128–130	118–122	179–182

Refer to Figure 1 for the structure abbreviations. The values in parentheses are coupling constants (*J*). d, doublet; t, triplet; dd, double doublet; dt, double triplet; m, multiplet; m.p., melting point; n.m., not measured because the compound was oily.

reaction time for compound **12S** was 45 min, in yields of 45.7 and 53.8%, respectively. ^{1}H and ^{13}C NMR data and m.p. are summarised in Table 3.

Results and discussion

Preparation of monolignol β-glycosides

A facile method for the synthesis of the monolignol β-glucopyranosides, coniferin (**1G**), syringin (**1S**), and *p*-glucocoumaryl alcohol (**1H**), has been reported by Terashima et al. (1996). This synthetic strategy consists of three major reactions, including a glycosylation, Knoevenagel condensation, and DIBAL-H mediated reduction, as shown in Figure 2. The glycosylation reaction is the key transformation in this particular sequence, because it proceeds in a stereoselective manner to afford the β-glycoside as a single product. The Koenigs-Knorr reaction is well-known as a useful method for the preparation of 1,2-*trans* glycosides, such as β-glucoside, β-galactoside, and β-xyloside, because of the neighboring group participation of the *O*-2 acyl groups, and this transformation was used for the glycosylation step in the synthesis of the monolignol β-glucosides (Terashima et al. 1996). The method for the construction of the monolignol glucosides (**1G**, **1S**, and **1H**) was then applied to the synthesis of the monolignol galactopyranosides (**2G**, **2S**, and **2H**) and the monolignol xylopyranosides (**3G**, **3S**, and **3H**). The synthesis of compound **2G** is described as a representative example, as follows. The glycosylation of vanillin (**13G**) with 2,3,4,6-tetra-*O*-acetyl-α-D-galactopyranosyl bromide (Pieber et al. 2010) (**17**) in the presence of Ag_2O in quinoline afforded the corresponding galactopyranoside (**18G**) in 97.7% yield. The ^{1}H NMR spectrum of the compound shows a peak at 5.11 ppm (doublet) with a coupling constant (*J*) of 7.5 Hz, whereas the ^{13}C NMR spectrum shows a peak at 99.7 ppm. These data indicated that compound **18G** was β-galactopyranoside. The subsequent condensation of compound **18G** with monoethyl malonic acid, which was prepared according to Hediger (2004), gave compound **19G**, which was reduced with DIBAL-H to give the target material **2G**. The ^{1}H NMR spectrum of compound **2G** was found to be in agreement with that of the previously reported material (Delay et al. 1994). Based on this result, it was therefore possible to obtain the target monolignol galactopyranosides (**2S** and **2H**) and monolignol xylopyranosides (**3G**, **3S** and **3H**) based on this method. It is important to note, however, that the reaction conditions in each case do not necessarily represent an optimised process.

Table 3 ^{1}H, ^{13}C NMR and m.p. data of *p*-hydroxybenzaldehyde derivative β-glycosides.

	9G	9S	9H	10G	10S	10H	11G	11S	11H	12G	12S	12H
^{1}H-NMR (ppm)												
H1	5.10 d (7.5)	5.20 d (7.5)	5.05 d (7.5)	5.05 d (7.5)	5.14 d (7.5)	5.00 d (7.5)	5.08 d (7.5)	5.14 d (6.5)	5.05 d (7.0)	5.25 s	5.07 d (0.5)	5.31 d (1.0)
H2	3.27–3.31	3.19–3.23	3.26–3.31	3.60–3.65	3.51–3.55	5.41 dt (2.0, 7.5)	3.22–3.28	3.30 m	3.24–3.28	3.88 d (4.0)	3.90 d (2.5)	3.88 s
H3	3.27–3.31	3.19–3.23	3.26–3.31	3.42–3.46	3.33–3.37	3.43 m	3.22–3.28	3.23 m	3.24–3.28	3.39–3.43	3.30 dd (3.0, 9.5)	3.40–3.43
H4	3.17 m	3.13 m	3.18 m	3.71 t (3.0)	3.65 t (3.5)	3.71 t (3.5)	3.33–3.39	3.36–3.40	3.39–3.41	3.39–3.43	3.35–3.39	3.40–3.43
H5a	3.39 m	3.07 m	3.40 m	3.60–3.65	3.28–3.32	3.64 t (6.0)	3.28–3.32	3.02 dd (9.0, 11.5)	3.35–3.38	3.29 m	3.00 m	3.30 m
H5b	–	–	–	–	–	–	3.74 dd (4.5, 10.5)	3.76 dd (5.0, 11.5)	3.76 dd (4.0, 9.5)	–	–	–
H6a	3.45 dt (6.0, 12.0)	3.39 dd (.0, 11.5)	3.47 dt (6.0, 12.0)	3.44–3.48	3.29–3.33	3.49 dd (5.5, 11.5)	–	–	–	3.46 dd (6.0, 12.0)	3.44 dd (6.0, 11.5)	3.46 dd (6.0, 11.5)
H6b	3.67 m	3.57 m	3.69 m	3.53 dt (5.5, 16.5)	3.47–3.51	3.55 dt (2.0, 7.5)	–	–	–	3.71 m	3.64 dd (2.0, 11.5)	3.72 dd (2.0, 12.0)
H2′	7.44 d (1.5)	7.25 s	7.87 d (8.5)	7.44 d (1.5)	7.25 s	7.87 d (9.0)	7.36 d (2.0)	7.25 s	7.87 d (8.5)	7.44 d (2.0)	7.27 s	7.86 d (8.5)
H3′	–	–	7.20 d (9.0)	–	–	7.20 d (9.0)	–	–	7.19 d (9.0)	–	–	7.17 d (8.5)
H5′	7.28 d (7.5)	–	7.20 d (9.0)	7.28 d (8.5)	–	7.20 d (9.0)	7.27 d (8.5)	–	7.19 d (9.0)	7.26 d (8.0)	–	7.17 d (8.5)
H6′	7.52 dd (1.5, 7.5)	7.25 s	7.87 d (8.5)	7.52 dd (2.0, 8.5)	7.25 s	7.87 d (9.0)	7.52 dd (1.5, 8.5)	7.25 s	7.87 d (8.5)	7.52 dd (2.0, 8.5)	7.27 s	7.86 d (8.5)
-OMe	3.84 s	3.84 s	–	3.84 s	3.84 s	–	3.84 s	3.84 s	–	3.84 s	3.86 s	–
-CHO	9.86 s	9.86 s	9.89 s	9.86 s	9.86 s	9.89 s	9.86 s	9.88 s	9.89 s	9.86 s	9.89 s	9.89 s
^{13}C-NMR (ppm)												
C1	99.3	101.8	99.7	100.0	102.5	100.3	100.1	102.4	100.2	97.8	101.3	97.2
C2	73.0	74.2	76.5	75.6	71.3	70.1	72.9	73.3	72.9	70.2	70.2	70.2
C3	76.8	76.6	73.1	73.5	73.3	73.2	76.6	75.4	76.3	73.4	73.4	73.3
C4	69.5	69.8	69.5	68.1	67.9	68.1	69.2	69.4	69.3	66.7	66.8	66.7
C5	77.1	77.5	77.1	75.6	75.7	75.7	65.8	65.6	65.8	77.9	78.0	77.8
C6	60.5	60.7	60.6	60.3	60.1	60.3	–	–	–	61.0	61.2	61.0
C1′	130.5	131.4	130.5	130.4	131.4	130.4	130.7	131.9	130.6	97.8	131.9	130.4
C2′	110.4	107.3	131.6	110.5	107.4	131.6	110.7	106.9	131.6	110.4	107.2	131.6
C3′	149.3	152.9	116.4	149.3	153.0	116.4	149.4	153.3	116.4	149.4	153.2	116.3
C4′	151.7	139.6	162.1	151.8	139.7	162.2	151.5	138.9	161.9	151.7	140.0	161.9
C5′	114.5	152.9	116.4	114.5	153.0	116.4	114.8	153.3	116.4	115.2	153.2	116.3
C6′	125.4	107.3	131.6	125.3	107.4	131.6	125.1	106.9	131.6	125.6	107.2	131.6

(**Table 3** Continued)

	9G	9S	9H	10G	10S	10H	11G	11S	11H	12G	12S	12H
-OMe	55.6	56.4	–	55.6	56.4	–	55.6	56.3	–	55.6	56.5	–
-CHO	191.5	191.8	191.5	191.5	191.8	191.5	191.5	191.9	191.5	191.5	191.9	191.5
m.p. (°C)	178–181	200–203	n.m.	179–184	194–195	165–168	n.m.	143–146	n.m.	166–169	n.m.	n.m.

Refer to Figure 1 for the structure abbreviations. The values in parentheses are coupling constants (*J*). d, doublet; t, triplet; dd, double doublet; dt, double triplet; m, multiplet; m.p., melting point; n.m., not measured because the compound was oily.

Then the synthesis of the monolignol β-mannopyranosides (**4G**, **4S**, and **4H**) was investigated. It is widely accepted that it is particularly difficult to achieve the selective synthesis of β-mannosides (i.e., 1,2-*cis* glycosides) because of the neighboring group participation of the *O*-2 acyl groups and the anomeric effect (Gridley and Osborn 2000). It is noteworthy that the Koenigs-Knorr method described above is not applicable for the synthesis of the β-mannosides. Cocinero et al. (2008) reported the synthesis of phenyl β-mannopyranoside in high yield based on a β-selective Mitsunobu glycosylation strategy. With this in mind, the application of a similar strategy was tested for the synthesis of the monolignol β-mannopyranosides (Figure 3). This, 2,3:4,6-di-*O*-isopropylidene- D-mannopyranose (**23**), which was prepared by the reaction of D-mannose with two equivalents of 2-methoxypropene in the presence of *p*-toluenesulfonic acid (Cocinero et al. 2008), was reacted with vanillin (**13G**) in presence of triphenylphosphine and DIAD to afford the corresponding mannoside as a mixture of the α- and β-anomers. Pleasingly, however, the α- and β-anomers (**24G**) were readily separated by a silica gel column chromatography, and obtained in 8.3 and 53.7% yields, respectively. The ratio of α- and β-anomers resulting from this reaction was determined to be 13:87. The configurations of the anomers were confirmed by ^{1}H and ^{13}C NMR spectroscopy. The α-configuration of the α-anomer was confirmed by the presence of a singlet peak in the ^{1}H NMR spectrum at 5.88 ppm, which was assigned to the $H_{1\alpha}$ proton, as well as a signal at 96.9 ppm in the ^{13}C NMR spectrum, which was assigned to the C_1 carbon. The $H_{1\alpha}$ signal was also reported as a singlet peak in the ^{1}H NMR spectra of phenyl 2,3:4,6-di-*O*-isopropylidene α-mannopyranoside (Cocinero et al. 2008), benzyl 2,3:4,6-di-*O*-isopropylidene α-mannopyranoside (Chung and Moon 1994), and methyl 2,3:4,6-di-*O*-isopropylidene α-mannopyranoside (Neogi et al. 2008). On the other hand, the β-configuration of the β-anomer (**24G**) was confirmed by the presence of a doublet with a *J* value of 3.5 Hz in its ^{1}H NMR spectrum at 5.62 ppm corresponding to the $H_{1\beta}$ proton, and a signal in the ^{13}C NMR at 96.6 ppm corresponding to the C_1 carbon. The subsequent Knoevenagel reaction of compound **24G** with monoethyl malonic acid, followed by the reduction of the resulting compound **25G** with DIBAL-H proceeded smoothly to give compound **26G**. Pleasingly, the isopropylidene rings of the mannoside were found to be stable under the both reaction conditions. Finally, compound **26G** was treated with an 80% AcOH aqueous solution to afford the target material **4G** in 69.1% yield. The signals corresponding to the isopropylidene moiety at 1.44, 1.56, and 1.63 ppm and 19.1, 25.9, 26.8, 29.0, 99.7, and 111.7 ppm,

respectively, disappeared in the ^{1}H and ^{13}C NMR spectra of compound **4G** (Figure 4), thus the removal of the isopropylidene groups was successful. The correlations derived from $C_{1\beta}$-$H_{1\beta}$ bonds of sugar moieties of compound **4G** appeared at δ_C/δ_H 100.3/5.01 ppm. On the other hand, Cocinero et al. (2008) reported that the correlation of phenyl β-mannoside appeared at different position (δ_C/δ_H 99.5/5.21 ppm), although the NMR solvent was MeOD. These results reconfirmed the importance of LCC model compounds. Compounds **4S** and **4H** were also prepared by the same method for compound **4G**.

Preparation of dihydromonolignol β-glycosides

Catalytic hydrogenation of monolignol β-glycosides (compounds **1G, 1S, 1H, 2G, 2S, 2H, 3G, 3S, 3H, 4G, 4S** and **4H**) were performed according to the conventional method to give the corresponding dihydromonolignol β-glycosides (compounds **5G, 5S, 5H, 6G, 6S, 6H, 7G, 7S, 7H, 8G, 8S** and **8H**), because dihydromonolignol β-glycosides are also important phenyl glycoside type LCC model compounds with C_{α}-C_{β} saturated substructures.

Preparation of *p*-hydroxybenzaldehyde derivative β-glycosides

C_{α}-oxidised substructures are present in native lignins (Adler and Marton 1959). Thus, *p*-hydroxybenzaldehyde derivative β-glycosides are also useful as the simplest phenyl glycoside type LCC model compounds with C_{α}-oxidised substructures. β-Glucoside (**15G**) was deacetylated to give compound **9G** in 94.9% yield. Compounds **15S, 15H, 18G, 18S, 18H, 21G, 21S** and **21H** were also converted to compounds **9S, 9H, 10G, 10S, 10H, 11G, 11S** and **11H** by the same method for **9G**. On the other hand, β-mannoside **24G** was deisopropylidenated to afford compound **12G** in 98.8% yield. Compounds **12S** and **12H** were also prepared based on the same method for **12G**.

NMR of β-glycosides of monolignol, dihydromonolignol and *p*-hydroxybenzaldehyde

The ^{1}H and ^{13}C NMR data in DMSO-d_6 of the compounds indicated are listed in Tables 1–3. The correlations derived from $C_{1\beta}$-$H_{1\beta}$ bonds of the sugar moieties of the all β-glycosides are summarised in Figure 5, in which several points remarkable. First, the correlations were varied and appeared in the range of δ_C/δ_H 97–100/4.9–5.4 ppm, suggesting that the assignment based on monolignol glucosides [coniferin (**1G**), syringin (**1S**) and *p*-glucocoumaryl alcohol (**1H**)] were insufficient in the literature (Balakshin et al. 2011; Yuan et al. 2011a; Miyagawa et al. 2013). Second, the $C_{1\beta}$-$H_{1\beta}$ signals of syringyl β-glycosides (**1S–12S**) appeared at a lower field compared with the guaiacyl (**1G–12G**) and *p*-hydroxyphenyl β-glycosides (**1H–12H**) in the ^{13}C NMR spectra, although no general correlation between the chemical shifts of $C_{1\beta}$-$H_{1\beta}$ bonds of the glycosides was noted. Third, the guaiacyl (**4G, 8G, 12G**) and *p*-hydroxyphenyl β-mannosides (**4H, 8H, 12H**) appeared at δ_C/δ_H 98.7/5.01, 99.0/4.93, 97.8/5.25, 97.7/5.12, 97.9/5.07 and 97.2/5.31 ppm, respectively, although it has been reported that the correlation of $C_{1\alpha}$-$H_{1\alpha}$ bonds of

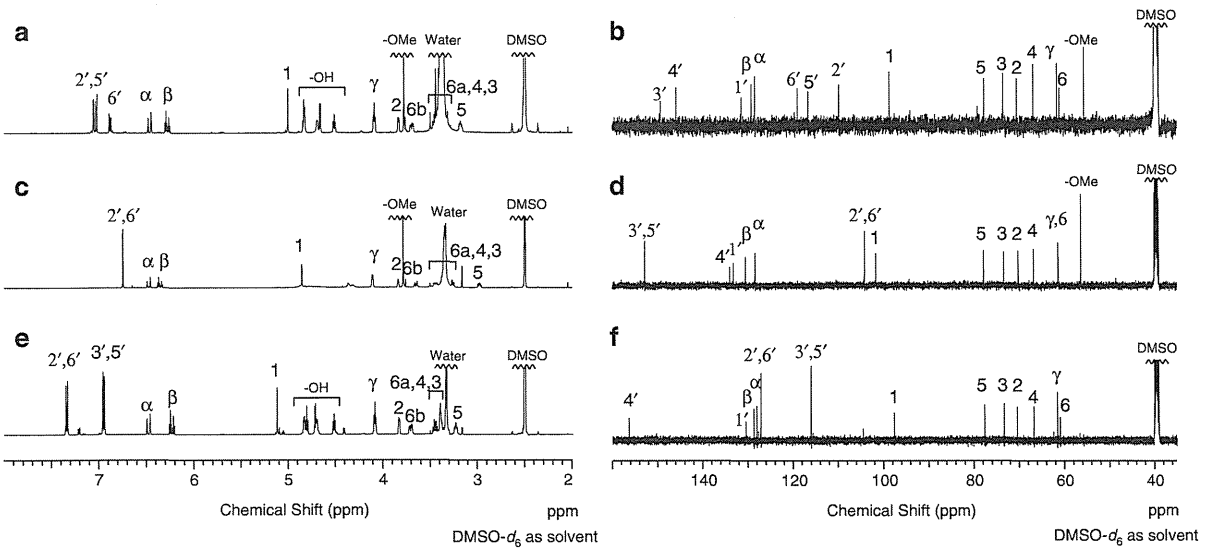

Figure 4 ^{1}H and ^{13}C-NMR spectra of monolignol β-mannosides **4G, 4S, 4H.** a and b: ^{1}H and ^{13}C-NMR spectra of compound **4G**; c and d: ^{1}H and ^{13}C-NMR spectra of compound **4S**; e and f: ^{1}H and ^{13}C-NMR spectra of compound **4H.**

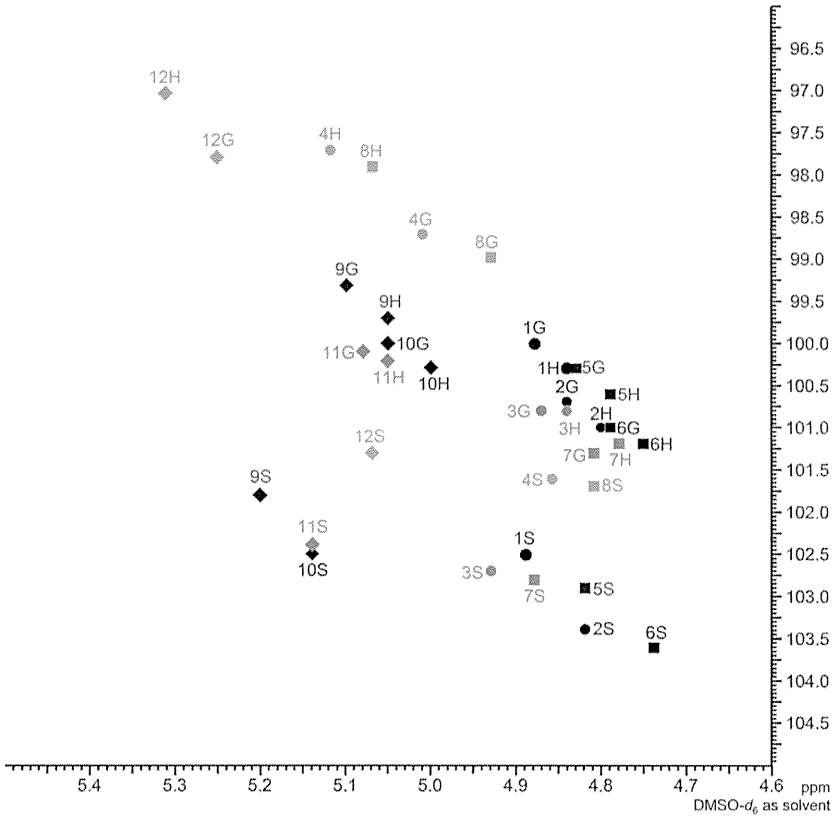

Figure 5 Correlations derived from $C_{1\beta}$-$H_{1\beta}$ of sugar moieties β-glycosides as model compounds of phenyl glycoside type LC linkages. Closed black circles: coniferin, syringin and *p*-glucocoumaryl alcohol; closed circles: monolignol β-glycosides; closed squares: dihydromonolignol β-glycosides; closed diamonds: *p*-hydroxybenzaldehyde derivative β-glycosides; red colour: β-glucosides; blue colour: β-galactosides; green colour: β-xylosides; orange colour: β-mannosides.

the 4-*O*-methyl-α-D-glucuronic acid moieties of hemicelluloses appeared around δ_C/δ_H 97/5.2 ppm (NMR solvent: $NaOD/D_2O$) in the previous paper (Teleman et al. 2002). In other words, the correlations derived from guaiacyl and *p*-hydroxyphenyl β-mannosides were located close to those that are thought to be derived from $C_{1\alpha}$-$H_{1\alpha}$ bonds of the 4-*O*-methyl-α-D-glucuronic acid moieties of hemicelluloses. Fourth, the correlations of dihydromonolignol β-glycosides were located close to those of the corresponding monolignol β-glycosides. These results show that the influences of the conjugation extended by C_α-C_β double bonds to the correlation of sugar moieties are small. Fifth, the correlation of *p*-hydroxybenzaldehyde derivative β-glycosides appeared far from those of the corresponding monolignol β-glycosides.

Unfortunately, the correlations in Figure 5 are not in perfect agreement with those that have been assigned to C_1-H_1 bonds of phenyl glycoside type LCCs in the previous papers (Balakshin et al. 2011; Yuan et al. 2011a; Miyagawa et al. 2013), but the correlation map (Figure 5) will be useful for analysis of C_1-H_1 bonds of phenyl glycoside type LCCs. We are currently investigating the syntheses of other phenyl glycoside LCC model compounds with more realistic lignin substructures.

Conclusions

Monolignol β-galactosides and β-xylosides were prepared according to the method for β-glucosides (Terashima et al. 1996), and the monolignol β-mannosides were also prepared based on Mitsunobu glycosylation (Cocinero et al. 2008). In addition, dihydromonolignol β-glycosides and *p*-hydroxybenzaldehyde derivative β-glycosides were also prepared from corresponding monolignol β-glycosides and the synthetic intermediates, respectively. Consequently, thirty six β-glycosides with different lignin moieties (monolignol, dihydromonolignol and *p*-hydroxybenzaldehyde derivative) and sugar moieties (D-glucose, D-galactose, D-xylose and D-mannose) were obtained as phenyl glycoside type LCCs model compounds, and subjected to HSQC NMR measurements. The correlations derived from $C_{1\beta}$-$H_{1\beta}$ bonds of sugar moieties of the all β-glycosides varied and were in the range of δ_C/δ_H

96–104/4.7–5.4 ppm. Furthermore, it was newly found that the correlations derived from $C_{1\beta}$-$H_{1\beta}$ bonds of guaiacyl and *p*-hydroxyphenyl β-mannosides (Compounds **4G**, **4H**, **8G**, **8H**, **12G** and **12H**) were close to those derived from the $C_{1\alpha}$-$H_{1\alpha}$ bonds of 4-*O*-methyl-α-D-glucuronic aid moieties described in the literature (Teleman et al. 2002), although the NMR solvent is different.

Received August 30, 2013; accepted January 27, 2014; previously published online February 21, 2014

References

Adler, E., Marton, J. (1959) Zur kenntnis der carbonylgruppen im Lignin. I. Acta Chem. Scand. 13:75–96.

Ando, D., Takano, T., Nakatsubo, F. (2012) Multi-steps degradation method for β-O-4 linkage in lignins: γ-TTSA method. Part 1: reaction of non-phenolic dimeric β-O-4 model compounds. Holzforschung 66:331–339.

Ando, D., Nakatsubo, F., Takano, T., Nishimura, H., Katahira, M., Yano, H. (2013) Multi-step degradation method for β-O-4 linkages in lignins: γ-TTSA method. Part 3. Degradation of milled wood lignin (MWL) from *Eucalyptus globulus*. Holzforschung 67:835–841.

Balakshin, M.Y., Capanema, E.A., Chang, H.-m. (2007) MWL fraction with a high concentration of lignin-carbohydrate linkages: isolation and 2D NMR spectroscopic analysis. Holzforschung 61:1–7.

Balakshin, M.Y., Capanema, E.A., Chang, H.M. (2008) Recent advances in the isolation and analysis of lignins and lignin-carbohydrate complexes. In: Characterization of Lignocellulosic Materials. Ed. Hu, T. Q. Blackwell Publishing Ltd., Oxford. pp. 148–170.

Balakshin, M., Capanema, E., Gracz, H., Chang, H.-m., Jameel, H. (2011) Quantification of lignin-carbohydrate linkages with high-resolution NMR spectroscopy. Planta 233:1097–1110.

Chung, S.-K., Moon, S.-H. (1994) Synthesis and biological activities of (4,6-di-*O*-phosphonato-β-D-mannopyranosyl)-methylphosphonate as an analogue of 1L-*myo*-inositol 1,4,5-trisphosphate. Carbohydr. Res. 260:39–50.

Cocinero, E.J., Stanca-Kaposta, E.C., Scanlan, E.M., Gamblin, D.P., Davis, B.G., Simons, J.P. (2008) Conformational choice and selectivity in singly and multiply hydrated monosaccharides in the gas phase. Chem. Eur. J. 14:8947–8955.

Daubresse, N., Francesch, C., Mhamdi, F., Rolando, C. (1998) Coniferin and derivatives. A fast and easy synthesis via the aldehyde series using phase-transfer catalysis. Synthesis 1998:157–161.

Delay, D., Dye, F., Wisniewski, J.P., Delmotte, F. (1994) Synthesis and Agrobacterium vir-inducing activities of coniferyl alcohol beta-glycosides. Phytochemistry 36:289–298.

Fengel, D., Wegener, G. (1983) Lignin-polysaccharide complexes. In: Wood, Chemistry, Ultrastructure, Reactions. Eds. Fengel, D., Wegener, G. Walter de Gruyter & Company, Berlin. pp. 167–174.

Gridley, J.J., Osborn, H.M. (2000) Recent advances in the construction of β-D-mannose and β-D-mannosamine linkages. J. Chem. Soc., Perkin Trans. 1. 2000:1471–1491.

Hediger, M.E. (2004) Design, synthesis, and evaluation of aza inhibitors of chorismate mutase. Bioorg. Med. Chem. 12:4995–5010.

Henriksson, G., Lawoko, M., Martin, M.E.E., Gellerstedt, G. (2007) Lignin-carbohydrate network in wood and pulps: a determinant for reactivity. Holzforschung 61:668–674.

Higuchi, R., Aritomi, M., Donnelly, D.M.X. (1977) Monolignol and dilignol glycosides from *Pinus contorta* leaves. Phytochemistry 16:1007–1011.

Jin, C., Micetich, R.G., Daneshtalab, M. (1999) Phenylpropanoid glycosides from *Stellera chamaejasme*. Phytochemistry 50: 677–680.

Kamel, M.S. (2003) Acylated phenolic glycosides from *Solenostemma argel*. Phytochemistry 62:1247–1250.

Kim, H., Ralph, J. (2010) Solution-state 2D NMR of ball-milled plant cell wall gels in DMSO-d_6/pyridine-d_5. Org. Biomol. Chem. 8:576–591.

Kim, H., Ralph, J, Akiyama, T. (2008) Solution-state 2D NMR of Ball-milled Plant Cell Wall Gels in DMSO-d_6. Bioenerg. Res. 1:56–66.

Koshijima, T., Watanabe, T. (2003) Analysis of native bonds between lignin and carbohydrate by specific chemical reactions. In: Association between Lignin and Carbohydrate in Wood and Other Plant Tissues. Ed. Timell, T.E. Springer, Berlin. pp. 91–30.

Lai, Y.-Z. (2001) Chemical degradation. In: Wood and Cellulosic Chemistry. second edition, revised and expanded. Eds. Hon, D.N.-S., Shiraishi, N. Marcel Dekker, Incorporated, New York. pp. 443–512.

Li, J., Martin-Sampedro, R., Pedrazzi, C., Gellerstedt, G. (2011) Fractionation and characterization of lignin-carbohydrate complexes (LCCs) from eucalyptus fibers. Holzforschung 65:43–50.

Machida, K., Sakamoto, S., Kikuchi, M. (2009) Two new neolignan glycosides from leaves of *Osmanthus heterophyllus*. J. Nat. Med. 63:227–231.

Mansfield, S.D., Kim, H., Lu, F., Ralph, J. (2012) Whole plant cell wall characterization using solution-state 2D NMR. Nat. Protoc. 7:1579–1589.

Mazur, M., Hope-Ross, K., Kadla, J.F., Sederoff, R., Chang, H.M. (2007) Synthesis of hydroxyphenylpropanoid beta-D-glucosides. J. Wood Chem. Technol. 27:1–8.

Miyagawa, Y., Takemoto, O., Takano, T., Kamitakahara, H., Nakatsubo, F. (2012) Fractionation and characterization of lignin carbohydrate complexes (LCCs) of *Eucalyptus globulus* in residues left after MWL isolation. Part I: analyses of hemicellulose-lignin fraction (HC-L). Holzforschung 66:459–465.

Miyagawa, Y., Kamitakahara, H., Takano, T. (2013) Fractionation and characterization of lignin carbohydrate complexes (LCCs) of *Eucalyptus globulus* in residues left after MWL isolation. Part II: Analyses of xylan-lignin fraction (X-L). Holzforschung 67:629–642.

Neogi, A., Majhi, T.P., Achari, B., Chattopadhyay, P. (2008) Palladium-catalyzed intramolecular C-O bond formation: An approach to the synthesis of chiral benzodioxocines. Eur. J. Org. Chem. 2008:330–336.

Pieber, B., Schober, S., Goebl, C., Mittelbach, M. (2010) Novel sensitive determination of steryl glycosides in biodiesel by gas chromatography-mass spectroscopy. J. Chrom. A. 1217: 6555–6561.

Ralph, J., Marita, J.M., Ralph, S.A., Hatfield, R.D., Lu, F., Ede, R.M., Peng, J., Quideau, S., Helm, R.F., Grabber, J.H., Kim, H., Jimenez-Monteon, G., Zhang, Y., Jung, H-J. G., Landucci, L.L., MacKay, J.J., Sederoff, R. R., Chapple, C., Boudet, A.M. (1999) Solution-state NMR of lignins. In: Advances in Lignocellulosics Characterization. Ed. Argyropoulos, D.S. Tappi Press. Atlanta, GA. pp. 55–108.

Ralph, S., Ralph, J., Landucci, L. (2004) NMR database of lignin and cell wall model compounds. http://ars.usda.gov/Services/docs.htm?docid=10491. Accessed on 28th August 2013.

Rencoret, J., Marques, G., Gutierrez, A., Nieto, L., Santos, J.I., Jimenez-Barbero, J., Martinez, A.T., del Rio, J.C. (2009) HSQC-NMR analysis of lignin in woody (*Eucalyptus globulus* and *Picea abies*) and non-woody (*Agave sisalana*) ball-milled plant materials at the gel state. Holzforschung 63:691–698.

Sugiyama, M., Nagayama, E., Kikuchi, M. (1993) Studies on the constituents of Osmanthus species. 14. Lignan and phenylpropanoid glycosides from *Osmanthus asiaticus*. Phytochemistry 33:1215–19.

Teleman, A., Tenkanen, M., Jacobs, A., Dahlman, O. (2002) Characterization of *O*-acetyl-(4-*O*-methylglucurono) xylan isolated from birch and beech. Carbohydr. Res. 337:373–377.

Terashima, N., Ralph, S.A., Landucci, L.L. (1996) New facile syntheses of monolignol glucosides; p-Glucocoumaryl alcohol, coniferin, and syringin. Holzforschung 50:151–155.

Westbye, P., Köhnke, T., Gatenholm, P. (2008) Fractionation and characterization of xylan rich extracts from birch. Holzforschung 62:31–37.

Yuan, T.-Q., Sun, S.-N., Xu, F., Sun, R.-C. (2011a) Characterization of lignin structures and Lignin-Carbohydrate Complex (LCC) linkages by quantitative ^{13}C and 2D HSQC NMR Spectroscopy. J. Agric. Food Chem. 59:10604–10614.

Yuan, T., Wan, C.P., Gonzalez-Sarrias, A., Kandhi, V., Cech, N.B., Seeram, N.P. (2011b) Phenolic glycosides from sugar maple (*Acer saccharum*) Bark. J. Nat. Prod. 74:2472–2476.

Cellulose (2014) 21:1885–1896
DOI 10.1007/s10570-014-0176-8

ORIGINAL PAPER

Preparation of Langmuir–Blodgett monolayer films of (zinc(II) phthalocyanine)-containing cellulose derivative; the use of 2,3-di-*O*-myristyl cellulose as a scaffold

Yasuko Saito · Hiroshi Kamitakahara · Toshiyuki Takano

Received: 31 July 2013 / Accepted: 20 January 2014 / Published online: 5 February 2014

Abstract The 6-*O*-phthalocyanine cellulose derivative, 2,3-di-*O*-myristyl-6-*O*-[*p*-(9(10),16(17),23(24)-tri-*tert*-butyl-2-zinc(II)phthalocyaninyl-benzoyl)cellulose (**8e**) was synthesized in a high yield with the degree of substitution of 0.33 for the phthalocyaninyl group ($DS_{phthalocyanine}$) via the esterification of 2,3-di-*O*-myristyl cellulose (**1**) with the *mono*-substituted phthalocyanine derivative ([9(10),16(17),23(24)-tri-*tert*-butyl-2-[4-(carboxy)phenoxy]phthalocyaninato] zinc(II), **7**). A chloroform solution of compound **8e** was more stable under illumination than that of low molecular weight phthalocyanine, [2(3),9(10),16(17), 23(24)-tetrakis(*tert*-butyl)phthalocyaninato]zinc(II). Langmuir–Blodgett (LB) monolayer films of compound **8e** were prepared on a variety of different substrates using the vertical dipping method with an annealing time of 5 min. An LB monolayer film of compound **8e** on an indium tin oxide (ITO) electrode exhibited a photocurrent generation performance in the range of 600–700 nm. The photocurrent density of the film composed of **8e** at 680 nm was better than that of 2,3-di-*O*-myristyl-6-*O*-(zinc(II) phthalocyaninyl) cellulose (**3**) which was the corresponding phthalocyanine-containing cellulose synthesized through a phthalocyanine-ring forming reaction on the cellulose backbone according to an existing procedure.

Keywords Cellulose · Langmuir–Blodgett film · Phthalocyanine · Phthalocyaninato zinc(II) · Regioselective · Photocurrent generation system

Introduction

Photosensitizer-bound cellulose derivatives are useful functional materials with potential applications in biomaterials-based solar cells. Indeed, Langmuir–Blodgett (LB) films constructed from 6-*O*-porphyrinyl-2,3-di-*O*-stearoyl cellulose and 6-*O*-porphyrinyl-2,3-di-*O*-myristoyl cellulose, have been reported to exhibit higher photocurrent generation performances (photon-to-electron conversion performances) around 430 nm than those of LB films from low molecular weight porphyrin molecules (Sakakibara et al. 2007; Sakakibara and Nakatsubo 2008, 2010). The high performances were thought to be due to high packing of the porphyrin moieties along the cellulose backbone without any aggregation, because it is well-known that the self-aggregation of porphyrin causes the remarkable decline of photocurrent generation performance

Electronic supplementary material The online version of this article (doi:10.1007/s10570-014-0176-8) contains supplementary material, which is available to authorized users.

Y. Saito (✉) · H. Kamitakahara · T. Takano
Division of Forest and Biomaterials Science, Graduate School of Agriculture, Kyoto University, Kitashirakawa-Oiwake-cho, Sakyo-ku, Kyoto 606-8502, Japan
e-mail: ysaito@kais.kyoto-u.ac.jp

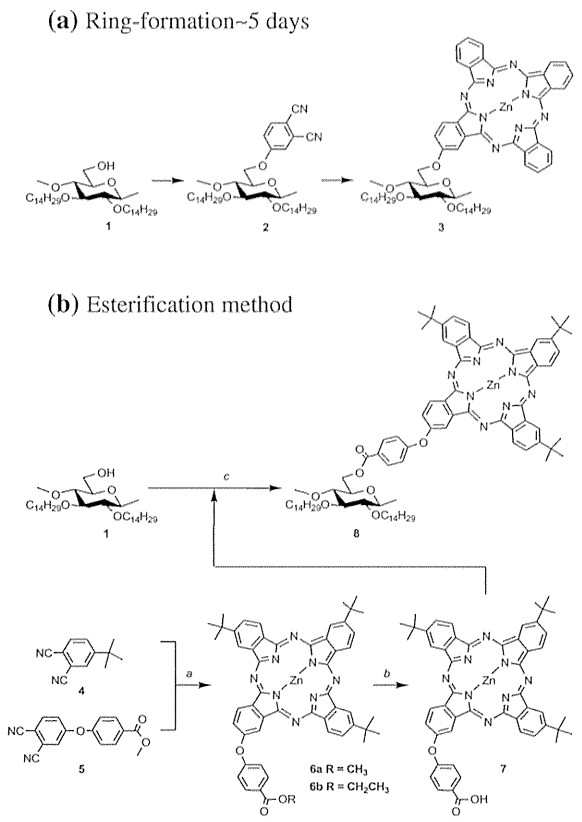

Fig. 1 Synthetic route for phthalocyanine-containing cellulose derivatives **3** (**a**) and **8** (**b**). **a** Ring-formation method [in the previous paper (Saito et al. 2012)]. **b** Esterification methods. *a*: $C(CH_3)_3$-C_6H_4-$(CN)_2$/$CH_3OCOC_6H_4O$-$C_6H_3(CN)_2$/$ZnCl_2$/DBN/EtOH/reflux/12 h. *b*: 1 M NaOHaq/THF/reflux/72 h. *c* Zn*t*BPc-COOH/EDC/DMAP/THF/50 °C/5 days

(Choudhury et al. 1998; Imahori et al. 2004). In other words, the cellulose backbone of the cellulose derivatives plays an important role in inhibiting the self-aggregation of the porphyrin moieties as scaffolds in the LB films. The effective utilization of solar light by the LB films has been limited, however, because the main absorption band of porphyrin (i.e., the Soret band) can be anywhere in the range of 400–450 nm (Sakakibara et al. 2007), whereas the target wavelength range for an ideal solar cell is generally considered to span the range of 300–1,200 nm (Burke et al. 2007). In our previous study, we reported the construction of an LB monolayer film of 2,3-di-*O*-myristyl-6-*O*-(zinc(II) phthalocyaninyl) cellulose (**3**) (Table 1) with the aim of moving into these otherwise unused wavelength ranges, except those associated with porphyrin adsorption (Saito et al. 2012). An LB monolayer film of compound **3** with a degree of substitution of 0.38 for the phthalocyaninyl groups ($DS_{phthalocyanine}$) showed photocurrent generation performance at 680 nm, but the performance was low. One of the reasons for the low photocurrent generation performance might be that the cellulose backbone of compound **3** did not inhibit the self-aggregation of the phthalocyanine moieties in the LB film sufficiently. Since compound **3** was synthesized by the phthalocyanine-ring formation reaction of 6-*O*-(3′,4′-dicyanophenyl)-2,3-di-*O*-myristyl cellulose (**2**) with a $DS_{dicyanophenyl}$ of 0.76 (Fig. 1a), it consequently contained unreacted dicyanophenyl groups and groups derived from the dicyanophenyl groups that had reacted with *O*-phthalodinitriles but did not form phthalocyanine-ring, except the phthalocyanine moieties with $DS_{phthalocyanine}$ of 0.38 at the *O*-6 position. Then, the packing of phthalocyanine moieties of compound **3** in the LB film might be disordered by the unwanted groups from the dicyanophenyl groups.

An alternative method for the preparation of phthalocyanine-containing cellulose derivatives involves the direct introduction of a *mono*-substituted phthalocyanine derivative to 2,3-di-*O*-myrstyl cellulose (**1**) (Fig. 1b). The advantage of this method is that only the phthalocyanine groups are introduced to the cellulose backbone of compound **1**, although the preparation of *mono*-substituted phthalocyanine derivatives can be time consuming (Erdem et al. 2008). The porphyrin-appended cellulose derivatives described above were also prepared by the direct esterification of the *mono*-substituted porphyrin derivatives (Sakakibara et al. 2007; Sakakibara and Nakatsubo 2008, 2010). In the current study, [9(10),16(17),23(24)-tri-*tert*-butyl-2-[(4-carboxy)phenoxy]phthalocyaninato]zinc(II) (Zn*t*BPc-COOH, **7**) was selected as the *mono*-substituted phthalocyanine derivative because of its good solubility profile in organic solvents, including chloroform and tetrahydrofuran (THF) (Mori et al. 2010), and then the phthalocyanine-containing cellulose derivative, that is, 2,3-di-*O*-myristyl-6-*O*-[*p*-(9(10),16(17),23(24)-tri-*tert*-butyl-2-zinc(II)phthalocyaninyl)-benzoyl]cellulose (**8**) was prepared via the direct esterification of compound **1** with Zn*t*BPc-COOH (**7**) (Fig. 1b) to improve the photocurrent generation performance of its LB monolayer film of compound **3**.

Experimental

Materials

2,3-Di-*O*-myristyl cellulose (**1**) with a $DS_{myristyl}$ of 1.64 (determined by elemental analysis) and a number-averaged degree of polymerization (DP_n) of 33 ($M_w/M_n = 1.56$) was prepared according to a previously reported procedure (Saito et al. 2012). [2(3),9(10),16(17),23(24)-Tetrakis(*tert*-butyl)phthalocyaninato]zinc(II) (Zn*t*BPc) was prepared according to the method of Mori et al. (2010) to be used as a reference sample for the UV–vis measurements. All of the other chemicals were purchased from commercial sources and used without further purification, unless otherwise specified. THF and chloroform were distilled from potassium and P_2O_5, respectively, prior to their use in the esterification reaction.

[9(10),16(17),23(24)-Tri-*tert*-butyl-2-[(4-carboxy)phenoxy]phthalocyaninato]zinc(II) (Zn*t*BPc-COOH, **7**)

4-*Tert*-butylphthalonitrile (**4**, 1.48 g, 8.03 mmol), 4-(4′-methoxycarbonyl)phenoxyphthalonitrile (**5**, 0.557 g, 2.00 mmol) which was prepared using the method described by Mori et al. (2010), $ZnCl_2$ (0.552 g, 4.05 mmol), and 1,5-diazabicyclo[4.3.0]non-5-ene (DBN) (1.5 mL, 12.1 mmol) were dissolved in ethanol (14.0 mL), and the resulting mixture was refluxed for 12 h. The mixture was then cooled and concentrated in vacuo to give the crude product as a residue, which was purified by sequential silica gel column chromatography (silica gel: Silica Gel 60 N (Kanto Chemical Co., Tokyo, Japan); eluent: dichloromethane) and preparative thin-layer chromatography (preparative TLC; silica gel plate made from Silica gel 60 PF254 (Merck, Darmstadt, Germany) with a thickness of 2 mm, eluent: dichloromethane) to afford a mixture of compounds **6a** and **6b** (0.203 g). The mixture was dissolved in THF (10 mL) before being treated with a 1 M aqueous NaOH solution (2.3 mL) and stirred under reflux for 72 h. The mixture was then cooled to ambient temperature and concentrated in vacuo to give a residue, which was suspended in distilled water (20 mL) and stirred under reflux for 1 h before being neutralized by the addition of acetic acid (0.13 mL, 2.3 mmol). The resulting precipitate was collected by filtration and dried in vacuo at ambient temperature to give compound **7** (0.193 g, 10.9 % yield) as a dark blue solid.

2,3-Di-*O*-myristyl-6-*O*-[*p*-(9(10),16(17),23(24)-tri-*tert*-butyl-2-zinc(II)phthalocyaninyl)-benzoyl]cellulose (**8e**)

Compound **7** (87.6 mg, 0.099 mmol), 1-ethyl-3-(3-dimethylaminopropyl)carbodiimide hydrochloride (EDC) (31.8 mg, 0.166 mmol), and 4-(dimethylamino)pyridine (DMAP) (19.6 mg, 0.160 mmol) were dissolved in anhydrous THF (0.5 mL), and the resulting mixture was stirred at ambient temperature for 30 min. A solution of 2,3-di-*O*-myristyl cellulose (**1**) (10.1 mg, 0.021 mmol) in THF (1.25 mL) was then added to the reaction in a drop-wise manner with constant stirring. The resulting mixture was then stirred at 50 °C for 5 days under an atmosphere of nitrogen, before being added to methanol (50 mL) in a drop-wise manner. The resulting precipitate was collected by centrifugation (14,000×*g*, 10 min) and washed with methanol, before being suspended in chloroform (5 mL). The suspension was then added to methanol (50 mL) in a drop-wise manner, and the resulting precipitate was collected by centrifugation (14,000×*g*, 10 min) and washed with methanol, before being suspended in chloroform (10 mL). The suspension was filtered to remove insoluble materials, and the filtrate was collected and added to methanol (50 mL) in a drop-wise manner. The resulting precipitate was collected by centrifugation (14,000×*g*, 10 min) and washed with methanol before being dissolved in chloroform (5 mL). The solution was then added to methanol (50 mL) in a drop-wise manner, and the resulting precipitate was collected by centrifugation (14,000×*g*, 10 min) and washed with methanol before being purified by gel filtration chromatography on a Sephadex LH-20 column (GE Healthcare, Tokyo, Japan) using 5 % methanol in chloroform (v/v) as the eluent to afford the 6-*O*-phthalocyanine-cellulose derivative **8e** (16.2 mg, ~100 %) as a dark blue solid.

Compound **8e**; $DS_{phthalocyanine}$: 0.33 (determined by the UV–vis method); DP_n: 21 ($M_w/M_n = 1.75$); ^1H NMR (chloroform-*d*): δ 9.84-6.76 (zinc(II) phthalocyaninyl-H, phenyl-H), 5.18-2.80 (cellulose ring-H, myristyl-OCH_2–), 2.46-0.55 (myristyl-CH_2–, and –CH_3, *tert*-butyl-CH_3) ppm; FT-IR (KBr): ν 3,435 (OH), 2,954, 2,924, 2,854, 1,724 (COO), 1,600, 1,485, 1,463 (C–H of AGU), 1,394, 1,365 (C–H of AGU), 1,323,

1,261, 1,238, 1,161, 1,089, 1,051, 939, 920, 833, 758 cm^{-1}; UV–vis (in chloroform): λ (log ε) 678 (4.3), 643 (4.2), 341 (4.3) nm.

Measurements

The FT-IR spectra were recorded from KBr pellets using a Shimadzu IRPrestige-21 spectrophotometer (Shimadzu Co., Kyoto, Japan). Matrix-assisted laser desorption/ionization time-of-flight mass (MALDI-TOF MS) spectra were recorded on a Bruker MALDI-TOF MS autoflex III (Bruker Daltonics, Bremen, Germany) using dithranol as a matrix in the positive ion and reflector modes with angiotensin II for external calibration. Gel permeation chromatography (GPC) was performed on a Shimadzu LC-10 system equipped with a Shimadzu UV–vis detector (SPD-10Avp) and a Shimadzu RI detector (RID-10A) under the following conditions. Columns: Shodex columns K-802, K-802.5, and K-805 connected in series (Showa Denko K. K., Tokyo, Japan); column temperature: 40 °C; eluent: chloroform; flow rate: 1.0 mL/min; standards: polystyrene standards (Shodex, Showa Denko K. K.). The ^{1}H NMR spectrum was recorded on a Varian 500 MHz FT-NMR (500 MHz) spectrometer (Agilent Technologies, Santa Clara, CA, USA) in chloroform-*d*. The chemical shift (δ) value have been given in parts per million (ppm). The UV–vis spectra were recorded on a Jasco V-560 UV–vis spectrophotometer (Jasco, Tokyo, Japan) in chloroform. The $DS_{phthalocyanine}$ of compound **8e** was estimated by UV–vis method (UV detection: 341 nm) with calibration curves from Zn*t*BPc (UV detection: 348 nm).

Photostability test of cellulose derivative **8e** in chloroform

Two separate solutions of compound **8e** in chloroform (0.05 mg/mL) were prepared. One was kept at 23 °C in the presence of light (under continuous illumination using a FHF32EX-N–H fluorescent lamp, Panasonic, Osaka, Japan), whereas the other was held at 23 °C in the absence of light (covered with aluminum foil). Samples of both solutions were collected and analyzed by UV–vis measurements in the range of 230–800 nm at the time points described in Fig. 5. Two separate solutions of Zn*t*BPc in chloroform (0.004 mg/mL) and those of compound **3** in chloroform (0.04 mg/mL) were prepared with almost same initial absorbance at 678 nm and subjected to the test conditions described above as controls.

Preparation of LB monolayer films of cellulose derivative **8e**

A solution of compound **8e** in chloroform (0.5 mg/mL) was spread onto a water subphase in a Teflon-coated trough (331 × 100 × 5 mm, USI-3-22T, USI-system, Fukuoka, Japan). The water used in the subphase was ultrapure water obtained from a Mili-Q water purification system (Merck, Millipore division, Tokyo, Japan). The solvent was evaporated over a period of 30 min and the surface pressure (π)–area (A) isotherms were measured at a constant compression rate of 6 mm/min. The surface pressure was measured using a Wilhelmy-type film balance. Prior to the deposition of the surface monolayer onto the substrates, the surface pressure was held at 10 mN/m for 5, 10, and 30 min. The vertical dipping method and horizontal lifting method were used to deposit the surface monolayers onto the substrates with an upward and downward stroke rate of 6 mm/min. The surface pressure was held at 10 mN/m throughout the deposition process, and the surface temperature was maintained at 20 °C to prepare the LB films. An LB film of compound **3** with a $DS_{phthalocyanine}$ of 0.38 and a DP_n of 25 ($M_w/M_n = 2.20$) was also prepared as a reference sample.

Characterization of the LB monolayer films of cellulose derivative **8e**

Polarized UV–vis spectra of the monolayer films were recorded on a Jasco V-560 UV–vis spectrophotometer equipped with a GPH-506 polarizer and RSH-680 revolving sample holder (Jasco, Tokyo, Japan). Observations of the monolayer films by atomic force microscopy (AFM) were performed in dynamic mode using a Shimadzu SPM-9600 AFM system (Shimadzu, Kyoto, Japan) equipped with a tetrahedral shaped silicon cantilever (AC240TS-C2, Olympus, Tokyo, Japan). Photocurrent measurements of the monolayer films were performed according to the method reported by Sakakibara and Nakatsubo (2010). Cyclic voltammograms (CVs) of the monolayer films were measured according to the method reported by Yang et al. (2003) using an electrochemical analyzer (ALS650B, BAS, Tokyo, Japan).

Table 1 List of acronyms and abbreviations

Compound 3	2,3-di-*O*-myristyl-6-*O*-(zinc(II) phthalocyaninyl) cellulose (6-*O*-phthalocyaninyl cellulose derivative synthesized via ring-formation reaction of phthalocyanine, See Fig. 1a)
Compound 8	2,3-di-*O*-myristyl-6-*O*-[*p*-(9(10),16(17),23(24)-tri-*tert*-butyl-2-zinc(II)phthalocyaninyl-benzoyl)cellulose (6-*O*-phthalocyaninyl cellulose derivative synthesized via esterification reaction, See Fig. 1b)
TPP-COOH	5-(4′-carboxyphenyl)-10,15,20-triphenylporphin
Zn*t*BPc	[2(3),9(10),16(17),23(24)-tetrakis(*tert*-butyl)phthalocyaninato]zinc(II)
Zn*t*BPc-COOH	*mono*-carboxylic acid of [2(3),9(10),16(17),23(24)-tetrakis(*tert*-butyl)phthalocyaninato]zinc(II)
AFM	atomic force microscopy
AGU	anhydroglucose unit
CV	cyclic voltammogram
DBN	1,5-diazabicyclo[4.3.0]non-5-ene
DCC	*N,N′*-dicyclohexylcarbodiimide
DMAP	4-(dimethylamino)pyridine
DS	degree of substitution
EDC	1-ethyl-3-(3-dimethylaminopropyl)carbodiimide
GPC	gel permeation chromatography
LB film	Langmuir–Blodgett film
THF	tetrahydrofuran
TLC	thin-layer chromatography

Results and discussion

Preparation of 2,3-di-*O*-myristyl-6-*O*-[*p*-(9(10),16(17),23(24)-tri-*tert*-butyl-2-phthalocyaninyl)-benzoyl] cellulose (**8**)

2,3-Di-*O*-myristyl cellulose (**1**) was synthesized from 6-*O*-(4-methoxytrityl)cellulose in 76.7 % yield using a previously reported procedure (Saito et al. 2012). Zn*t*BPc-COOH (**7**) was prepared according to a modified version of the method reported by Mori et al. (2010) where ethanol was used instead of *n*-pentanol as the solvent for the phthalocyanine-ring forming reaction. The phthalocyanine-ring forming reaction between 4-*tert*-butylphthalonitrile (**4**) and 4-(4′-methoxycarbonyl)phenoxyphthalonitrile (**5**) was conducted in ethanol under reflux over a period of 12 h to afford a crude product mixture of *mono*-substituted phthalocyanine derivatives (**6a**: methyl ester and **6b**: ethyl ester), which were isolated from the other products by silica gel column chromatography followed by preparative TLC. In contrast, the purification of the corresponding *mono*-substituted phthalocyanine derivative (*n*-pentyl ester) by the same reaction in *n*-pentanol was achieved by active alumina column chromatography followed by preparative high-performance liquid chromatography in the literature (Mori et al. 2010). The use of ethanol as a solvent contributed to the easier purification of *mono*-substituted phthalocyanine derivatives **6a** and **6b**. Subsequent base-mediated hydrolysis of the mixture of compounds **6a** and **6b** with a 1 M aqueous NaOH solution under reflux for 72 h gave Zn*t*BPc-COOH (**7**) in 10.9 % yield. The FT-IR and MALDI-TOF MS spectra of compound **7** were in good agreement with those reported in the literature (data not shown) (Cid et al. 2009; Mori et al. 2010).

Sakakibara et al. (2007) reported that the reaction of 2,3-di-*O*-stearoyl cellulose with a *mono*-porphyrin carboxylic acid derivative (TPP-COOH) in dichloromethane at ambient temperature over a period of 5 days in the presence of *N,N′*-dicyclohexylcarbodiimide (DCC) and DMAP gave a porphyrin-containing cellulose derivative with a $DS_{porphyrin}$ of 0.64 in 90 % yield. With this in mind, compound **1** was treated with Zn*t*BPc-COOH (**7**) in chloroform at ambient temperature for 5 days in the presence of DCC and DMAP to afford compound **8a** (Entry a in Table 2). Chloroform was used as a solvent instead of dichloromethane because compound **1** was more soluble in chloroform.

The $DS_{phthalocyanine}$ of compound **3** was estimated using the UV–vis method (detection wavelength: 676 nm) in the previous paper (Saito et al. 2012).

Table 2 Esterification conditions of compound **1**[a]

Entry	Zn*t*BPc-COOH (eq)	Condensing agent	Solvent	Temperature (°C)	Product	$^{b}_{\text{phthalocyanine}}$	Yield (%)
a	4	DCC	$CHCl_3$	r.t.	8a	0.07	89.0
b	4	DCC	THF	r.t.	8b	0.03	96.2
c	4	EDC	THF	r.t.	8c	0.16	78.3
d	5	EDC	THF	r.t.	8d	0.38	93.5
e	5	EDC	THF	50	8c	0.33	~100

[a] Reaction time was 5 days

[b] Determined by UV-vis method (detection wavelength: 341 nm)

But, it was newly found that the Q bands might be influenced by the aggregation of compound **3**. Then, the $DS_{phthalocyanine}$ of compound **8** was estimated by the UV–vis method using Soret bands (detection wavelength: 341 nm) together with the calibration curves from Zn*t*BPc. The $DS_{phthalocyanine}$ of compound **8a** was found to be only 0.07. Redl et al. (2001) reported the formation of a porphyrin-containing cellulose derivative with a $DS_{porphyrin}$ of 0.43 in 32 % yield following the reaction of 2,3-di-*O*-methyl cellulose with TPP-COOH in the presence of EDC and DMAP in a mixture of pentafluorophenol and THF at ambient temperature for 5 days, followed by 4 days of heating under reflux, and an additional week at ambient temperature. When we applied this methodology to the current problem, THF was used as the solvent instead of chloroform. Unfortunately, however, this led to a reduction in the $DS_{phthalocyanine}$ of compound **8b** (Entry b). The use of EDC as a condensation reagent instead of DCC was also investigated in the current study. The esterification of compound **1** with Zn*t*BPc-COOH (**7**) in the presence of EDC system afforded compound **8** with a higher $DS_{phthalocyanine}$ value than the corresponding esterification reaction with Zn*t*BPc-COOH (**7**) using the DCC system (Entries b and c, respectively). When the amount of Zn*t*BPc-COOH (**7**) was increased, the $DS_{phthalocyanine}$ of compound **8** also increased (Entry d). Investigation of the reaction temperature revealed that this parameter contributed to higher yield of compound **8** although it did not exert any influence over the $DS_{phthalocyanine}$ of compound **8** (Entry e). Consequently, the highest $DS_{phthalocyanine}$ value and yield observed for compound **8** were 0.38 (Entry d) and ~100 % yield (Entry e), respectively. Compound **8e** was subjected to GPC, FT-IR, NMR, and UV–vis analyses. Figure 2 shows the GPC elution curves of

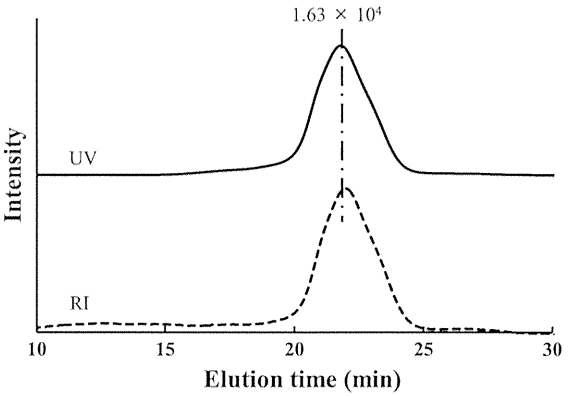

Fig. 2 GPC elution curves of compound **8e** (UV detection wavelength was 600 nm)

compound **8e**. The peak corresponding to Zn*t*BPc-COOH (**7**) around 26 min was absent from the UV elution curve of compound **8e**, suggesting that Zn*t*BPc-COOH (**7**) had been completely removed from the material as a consequence of the extensive purification process for compound **8e**. The FT-IR spectrum of compound **8e** (Fig. 3b) revealed that the characteristic bands assigned to the cellulose backbone at 1,463, 1,365, and 1,040–1,100 cm^{-1} (Fig. 3a), as well as those assigned to the Zn(II) phthalocyanine ring at 1,600, 1,485, 1,394, 1,323, 1,238, 1,161, 1,089, 1,051, and 758 cm^{-1} (Fig. 3c) (Cid et al. 2009) were all present. A new band derived from the ester group at 1,724 cm^{-1} (Shirai et al. 1984) was also observed, indicating the formation of the ester link. This suggestion was also supported by ^{1}H NMR and UV–vis data. The broad signals in the range of 5.18–2.80 ppm of the ^{1}H NMR spectrum of **8e** were derived from protons of the cellulose ring, whereas the signals in the range of 9.84–6.76 ppm were derived from aromatic protons of the phthalocyanine (Fig. S1

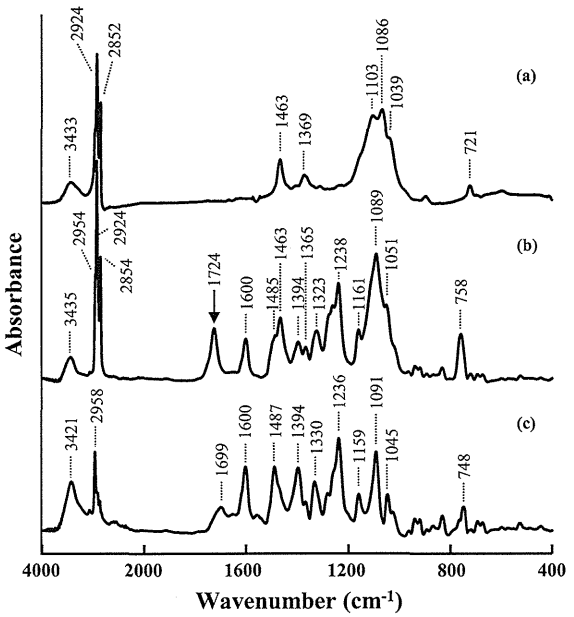

Fig. 3 FT-IR spectra of compounds **1**: (**a**), **8e**: (**b**) and **7**: (**c**)

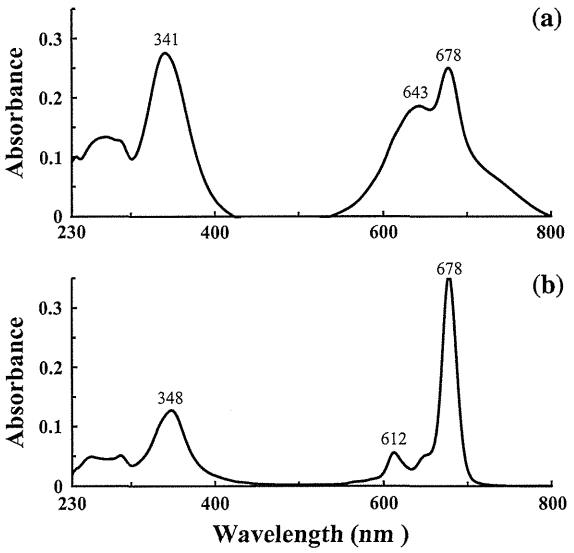

Fig. 4 UV–vis spectra of compounds **8e** (0.01 mg/mL): (**a**), Zn*t*BPc (2×10^{-6} M): (**b**) in $CHCl_3$

of the Supporting Information). The Soret bands were clearly observed in the UV–vis spectra of compound **8e** (Fig. 4a) and Zn*t*BPc (Fig. 4b) in the range of 300–400 nm, the Q bands of these compounds were observed in the same spectra in the range of 600–700 nm. Furthermore, in Fig. 2, the RI and UV elution curves of compound **8e** provided identical elution profiles. These results effectively reconfirmed that the cellulose backbone was bonded to the phthalocyanine moieties in compound **8e**. The $DS_{phthalocyanine}$ of compound **8e** was found to be 0.33 by the UV–vis method described above. The intensities of the two bands at 643 and 678 nm in the Q bands of compound **8e** were almost identical (Fig. 4a) and differed from those in the UV–vis spectrum of Zn*t*BPc (Fig. 4b), suggesting that some of the phthalocyanine units had aggregated in the chloroform solution of compound **8e** (Allcock and Neenan 1986). Finally, the DP_n of compound **8e** was calculated using the following Eq. (1).

$$DP_n = M_n(1.63 \times 10^4) / [(\text{a phthalocyanine - containing unit}\,(1,348)) * 0.33 + (\text{a unit without phthalocyanine}\,(483)) * 0.67] \quad (1)$$

The DP_n of compound **8e** was decreased from 33 to 21 during esterification. Despite of depolymerization of cellulose backbone, the yield of compound **8e** was ~100 %. The value seemed to be higher than a real one. One possibility might be that unreacted Zn*t*BPc-COOH aggregates the phthalocyanine moieties of compound **8e** tightly even after an extensive reaction work-up procedure, although further investigations were required.

Photostability test of cellulose derivative **8e** in chloroform

Numerous different studies have appeared in the literature indicating that the photostabilities of phthalocyanines in a variety of different solvents under illumination are generally low (Sobbi et al. 1993; Stota and Dyrda 2003; Isago et al. 2008). For example, [2(3),9(10),16(17),23(24)-teirakis(*tert*-butyl)phthalocyaninato]antimony(III) in aerated chloroform was reported to be bleached after 252 min under irradiation with visible light (Isago et al. 2008). The photostabilities of the chloroform solutions of compound **8e** and controls (compound **3** and Zn*t*BPc) were investigated. Changes in the absorbance properties of the compound **8e** solution at 678 nm, and Zn*t*BPc solution at 678 nm, and in that of the compound **3** solution at 676 nm in the presence and absence of light are shown in Fig. 5. When the chloroform solutions of